A Raman spectroscopic study of copiapites $Fe^{2+}Fe^{3+}(SO_4)_6(OH)_2{\cdot}20H_2O$ -environmental implications

Ray L. Frost •

Chemistry, Faculty of Science and Technology, Queensland University of Technology, GPO Box 2434, Brisbane Queensland 4001, Australia.

ABSTRACT

Raman spectroscopy has been used to study selected mineral samples of the copiapites group. Copiapite $Fe^{2+}Fe^{3+}(SO_4)_6(OH)_2{\cdot}20H_2O$ is a secondary mineral formed through the oxidation of pyrite. Minerals of the copiapite group have a general formula of $AFe_4(SO_4)_6(OH)_2 \cdot 20H_2O$, where A has a positive 2 charge and can be either magnesium, iron, copper, calcium and/or zinc. The formula can also be $B_{2/3}Fe_4(SO_4)_6(OH)_2{\cdot}20H_2O$, where B has a positive 3 charge and may be either aluminium or iron. For each mineral two Raman bands are observed at around 992 and 1029 cm^{-1}, assigned to the $(SO_4)^{2-}$ ν_1 symmetric stretching mode. The observation of two bands provides evidence for the existence of two non-equivalent sulphate anions in the mineral structure. Three Raman bands at 1112, 1142 and 1161 cm^{-1} are observed in the Raman spectrum of copiapites, indicating a reduction of symmetry of the sulphate anion in the copiapites structure. This reduction in symmetry is supported by multiple bands in the ν_2 and ν_4 $(SO_4)^{2-}$ spectral regions.

KEYWORDS: copiapites, sulphate, Raman spectroscopy, reduction in symmetry, environmental implications

• Author to whom correspondence should be addressed (r.frost@qut.edu.au)

INTRODUCTION

Copiapite $Fe^{2+}Fe^{3+}(SO_4)_6(OH)_2{\cdot}20H_2O$ [1-4] is a secondary mineral formed through the oxidation of pyrite. The mineral was named for the famed mineral locality at Copiapo, Chile which is where it was first discovered. It is difficult to distinguish copiapite from other similar hydrated iron sulphates without X-ray studies. Copiapite lends its name to a group of similar triclinic, hydrated, iron sulphates called the copiapite group. The members of this group are all distinct minerals. The general formula of this group is $AFe_4(SO_4)_6(OH)_2 \cdot 20H_2O$, where A has a positive 2 charge and can be either magnesium, iron, copper, calcium and/or zinc. The formula can also be $B_{2/3}Fe_4(SO_4)_6(OH)_2{\cdot}20H_2O$, where B has a positive 3 charge and may be either aluminium or iron. Mineral members of this group include copiapite (hydrated iron magnesium sulphate hydroxide) [1, 5, 6], ferricopiapite (hydrated iron sulphate hydroxide)[5], magnesiocopiapite (hydrated magnesium iron sulphate hydroxide), zincocopiapite (hydrated zinc iron sulphate hydroxide). Other members include aluminocopiapite (hydrated aluminium iron sulphate hydroxide), calciocopiapite (hydrated calcium iron sulphate hydroxide), cuprocopiapite (hydrated copper iron sulphate hydroxide) [7]. The minerals are a sulphur yellow colour and may be confused for secondary uranyl minerals [8-11]. Indeed the copiapites minerals are often found in the same deposits as these uranyl minerals.

Copiapite is a mineral of environmental significance [12]. The mineral is involved in many paragenetic relationships and solid solutions involving the above mentioned minerals are common [12]. Williams defined the phase diagram for stability of iron sulphate minerals and copiapites has a well defined primary phase field [12]. The mineral is formed in efflorescent deposits [13, 14]. The mineral copiapite is often found in slag heaps [13, 15-18] and may be found in coal mines [19]. The copiapites and related minerals are used to model the Martian surface [20]. It is important to study sulphate minerals including copiapites as their presence may be/will be detected on Mars. Intense research is being focussed on the design of portable-type Raman spectrometers which at some future time will be sent to Mars. Raman spectroscopy is going to be of great importance for the determination of minerals on Mars. Copiapites are minerals formed from solutions; so their presence on the Mars surface would imply that water existed at some previous time and that solutions flowed across the surface of Mars. The significance of a Mars Raman microprobe is that the instrument will be able to determine very small crystals. Whilst some infrared studies of sulphate minerals have been undertaken [21, 22], few

Raman studies of such copiapites minerals have been undertaken. As part of our on-going studies of the vibrational spectroscopy of minerals particularly secondary minerals, we report the Raman spectra of the copiapites minerals. The Raman spectra are related to the molecular structure of copiapite.

EXPERIMENTAL

Minerals

Copiapite originated from Alcaparrosa mine, Tierra Amarilla, Chile; ferricopiapite from Alcaparrosa mine, near Cerritos Bayos, El Loa Province, Chile; magnesiocopiapite from the Denver mine, Santa Cruz County, Arizona, USA; zincocopiapite originated from Les Valettes, Wallis, Switzerland.

Raman spectroscopy

Crystals of copiapites or cation substituted copiapite were placed on a polished metal surface on the stage of an Olympus BHSM microscope, which is equipped with 10x, 20x, and 50x objectives. The microscope is part of a Renishaw 1000 Raman microscope system, which also includes a monochromator, a filter system and a CCD detector (1024 pixels). The Raman spectra were excited by a Spectra-Physics model 127 He-Ne laser producing highly polarised light at 633 nm and collected at a nominal resolution of 2 cm^{-1} and a precision of ± 1 cm^{-1} in the range between 200 and 4000 cm^{-1}. Repeated acquisition on the crystals using the highest magnification (50x) were accumulated to improve the signal to noise ratio in the spectra. Spectra were calibrated using the 520.5 cm^{-1} line of a silicon wafer. Previous studies by the authors provide more details of the experimental technique. [23-26]

Spectral manipulation such as baseline correction/adjustment and smoothing were performed using the Spectracalc software package GRAMS (Galactic Industries Corporation, NH, USA). Band component analysis was undertaken using the Jandel 'Peakfit' software

package that enabled the type of fitting function to be selected and allows specific parameters to be fixed or varied accordingly. Band fitting was done using a Lorentzian-Gaussian cross-product function with the minimum number of component bands used for the fitting process. The Gaussian-Lorentzian ratio was maintained at values greater than 0.7 and fitting was undertaken until reproducible results were obtained with squared correlations of r^2 greater than 0.995.

RESULTS AND DISCUSSION

Background spectroscopy of sulphate

The Raman spectroscopy of the aqueous sulphate tetrahedral oxyanion yields the symmetric stretching (ν_1) vibration at 981 cm^{-1}, the in-plane bending (ν_2) mode at 451 cm^{-1}, the antisymmetric stretching (ν_3) mode at 1104 cm^{-1} and the out-of-plane bending (ν_4) mode at 613 cm^{-1} [27]. Ross reports the interpretation of the infrared spectra for potassium alum as ν_1, 981 cm^{-1}; ν_2, 465 cm^{-1}; ν_3, 1200, 1105 cm^{-1}; ν_4, 618 and 600 cm^{-1} [28]. Water stretching modes were reported at 3400 and 3000 cm^{-1}, bending modes at 1645 cm^{-1}, and librational modes at 930 and 700 cm^{-1} [29]. The Raman spectrum of the mineral chalcanthite shows a single symmetric stretching mode at 984.7 cm^{-1}. Two ν_2 modes are observed at 463 and 445 cm^{-1} and three ν_3 modes at 1173, 1146 and 1100 cm^{-1}. The ν_4 mode is observed as a single band at 610 cm^{-1}. A complex set of overlapping bands is observed in the low wavenumber region at 257, 244, 210 136 and 126 cm^{-1}. Recently, Raman spectra of four basic copper sulphate minerals, namely antlerite, brochiantite, posnjakite and langite, were published [30]. The SO symmetric stretching modes for the four basic copper sulphate minerals are observed at 985, 990, 972 and 974 cm^{-1}. Multiple bands were observed for these minerals in the antisymmetric stretching region.

Ross also lists the infrared spectra of the pseudo-alums formed from one divalent and one trivalent cations. Halotrichite has infrared bands at ν_1, 1000 cm^{-1}; ν_2, 480 cm^{-1}; ν_3, 1121, 1085, 1068 cm^{-1}; ν_4, 645, 600 cm^{-1}. Pickeringite the Mg end member of the halotrichite-pickeringite series has infrared bands at ν_1, 1000 cm^{-1}; ν_2, 435 cm^{-1}; ν_3, 1085, 1025 cm^{-1}; ν_4, 638, 600 cm^{-1} [28]. These minerals display infrared water bands in the OH stretching, 3400 and

3000 cm^{-1} region; OH deformation, 1650 cm^{-1} region; OH libration, 725 cm^{-1} region. Ross also reports a weak band at ~960 cm^{-1} which is assigned to a second OH librational vibration [28]. As with the infrared spectra, Raman spectra of alums are based on the combination of the spectra of the sulphate and water. Sulphate typically is a tetrahedral oxyanion with Raman bands at 981 (ν_1), 451 (ν_2), 1104 (ν_3) and 613 (ν_4) cm^{-1} [31]. Some sulphates have their symmetry reduced through acting as monodentate and bidentate ligands [31]. In the case of bidentate behaviour both bridging and chelating ligands are known. This reduction in symmetry is observed by the splitting of the ν_3 and ν_4 into two components under C_{3v} symmetry and 3 components under C_{2v} symmetry. A complex set of overlapping bands is observed in the low wavenumber region with broad bands observed at 257, 244, 210 136 and 126 cm^{-1}.

Raman spectroscopy

The Raman spectra of copiapites, ferricopiapite, magnesiocopiapite and zincocopiapite in the 700 to 1300 cm^{-1} region are shown in Figs. 1 to 4 respectively and the Raman spectra of copiapites, ferricopiapite, magnesiocopiapite and zincocopiapite in the 100 to 700 cm^{-1} region are shown in Figs. 5 to 8 respectively.

The Raman spectrum of copiapite displays two distinct bands at 998 and 1029 cm^{-1}. These two bands are assigned to the $(SO_4)^{2-}$ ν_1 symmetric stretching mode. These bands are observed at 992 and 1019 cm^{-1} for ferricopiapite, 995 and 1028 cm^{-1} for magnesiocopiapite and 1005 and 1021 cm^{-1} for the zincocopiapite. The significance of the multiple bands in the symmetric region provides evidence for the non-equivalence of sulphate units in the copiapite structure. Differences in the peak positions are attributed to the size of the cation and the polarizing power of that cation. The cations with a weaker polarising power such as Zn cause the sulphate bands to be found at higher wavenumbers. The cations with stronger polarising power have bands at lower wavenumbers. Raman bands are observed at 1112, 1142 and 1161 cm^{-1} in the Raman spectrum of copiapites. These bands are assigned to the $(SO_4)^{2-}$ ν_3 antisymmetric stretching modes. The bands are more clearly resolved for ferricopiapite and three Raman bands are found at 1105, 1124 and 1147 cm^{-1} attributed to the $(SO_4)^{2-}$ ν_3 antisymmetric stretching vibrations. For the magnesiocopiapite the bands are observed at 1114, 1146 and 1165 cm^{-1} with an additional band at 1244 cm^{-1}. For the zincocopiapite,

160 Raman bands are found at 1099, 1159, 1162 and 1231 cm^{-1}. The significance of these
161 multiple antisymmetric stretching modes proves the symmetry of the sulphate anion in the
162 copiapite structure is reduced from T_d to C_{3v} or even C_{2v}.
163
164 Two low intensity bands for ferricopiapites are found at 754 and 843 cm^{-1}. The first
165 band is assigned to the FeOH deformation vibration and the latter band to a water librational
166 mode. Water librational bands are normally of very low intensity in the Raman spectrum but
167 are usually intense in the infrared spectrum. The bands are of very low intensity in the
168 Raman spectrum of copiapites; a band may be observed at around 740 cm^{-1}. Two bands are
169 observed in the Raman spectrum of magnesiocopiapite at 753 and 884 cm^{-1}. Three Raman
170 bands are observed for the zincocopiapite at 738, 860 and 893 cm^{-1}. The first band is
171 assigned to the FeOH deformation mode and the latter two bands to water librational modes.
172
173 A series of low intensity bands are observed in the Raman spectrum of copiapites at
174 553, 595, 615 and 639 cm^{-1}. These bands are assigned to the $\nu_4 (SO_4)^{2-}$ bending modes. The
175 bands are more clearly observed in the Raman spectrum of ferricopiapite at 554, 599, 612 and
176 638 cm^{-1}. The Raman bands are observed at 555, 610 and 639 cm^{-1} for magnesiocopiapite.
177 The Raman bands are found at 565, 613 and 624 cm^{-1} for zincocopiapite. The observation of
178 multiple bands in this spectral region offers evidence for the reduction in symmetry of the
179 sulphate anion from T_d to C_{2v} or even lower symmetry. Raman bands at 426, 450 and 476
180 cm^{-1} for copiapite are assigned to the $\nu_2 (SO_4)^{2-}$ bending modes. For ferricopiapite, the Raman
181 bands are found at 401, 451 and 481 cm^{-1}; for magnesiocopiapite the bands are found at 412,
182 446 and 474 cm^{-1} and for zincocopiapite the bands are more clearly resolved and are
183 observed at 424, 450 and 485 cm^{-1}. For each of these minerals three bands are observed.
184 The observation of multiple bands supports the concept of the reduction of the symmetry of
185 the sulphate anion.
186
187 **Environmental implications**
188
189 Copiapites are simply one of a group of ferrous/ferric minerals which may be termed
190 'environmental' minerals. These minerals include hydronium jarosites, butlerite/parabutlerite,
191 coquimbite, roemerite and the hydrated ferrous sulphate minerals 97 in total). All these
192 minerals are formed as a result of the oxidation of pyrite and are a result of the crystallisation

from solution. The significance of the Raman spectra of copiapites lies with the ability to determine small crystals down to around 1 micron. The fact that copiapites are found is an indication of acid-sulphate soils. Complex equilibria exist in solution which are dependent upon the temperature, vapour pressure and concentrations of acid and the ferrous and ferric ions. The formation of copiapites and related minerals provides evidence of environmental impact. These minerals are formed in metallurgical waste dumps [13]. The minerals provide an indication of weathering [32]. Such minerals are formed from mine tailings and may serve to soak up heavy metals [33]. Such minerals are found in sulphated soils [34]. Formation of the copiapites provide an indication of the lack of remediation of old mine sites [35]. The copiapites are significant indicators of acid mine drainage [36].

CONCLUSIONS

The Raman spectra of selected copiapites $Fe^{2+}Fe^{3+}(SO_4)_6(OH)_2{\cdot}20H_2O$ have been undertaken and the spectra related to the mineral structure. Two Raman bands are observed at around 992 and 1029 cm^{-1}, assigned to the $(SO_4)^{2-}$ ν_1 symmetric stretching mode. The observation of two bands provides evidence for the existence of two non-equivalent sulphate anions in the mineral structure. Three Raman bands at 1112, 1142 and 1161 cm^{-1} are observed indicating a reduction of symmetry of the sulphate anion in the copiapites structure. This reduction in symmetry is supported by multiple bands in the ν_2 and ν_4 $(SO_4)^{2-}$ spectral regions.

Copiapites are simply one of a group of ferrous/ferric minerals which may be termed 'environmental' minerals. These minerals are formed as a result of the oxidation of pyrite and are a result of the crystallisation from solution. Complex equilibria exist in solution that are dependent upon the temperature, vapour pressure and concentrations of acid and the ferrous and ferric ions. The formation of copiapites and related minerals provides evidence of environmental impact.

Acknowledgements

The financial and infra-structure support of the Queensland University of Technology Inorganic Materials Research Program is gratefully acknowledged. The Australian Research Council (ARC) is thanked for funding the instrumentation.

References

[1] P. Bayliss, D. Atencio, *Can. Min.* **1985,** *23,* 53-56.

[2] C. Palache, M. A. Peacock, L. G. Berry, *University of Toronto Studies, Geological Series* **1946,** *No. 50,* 9-26.

[3] P. Suesse, *Neues Jahrbuch fuer Mineralogie, Monatshefte* **1970,** 286-287.

[4] P. Suesse, *Z. Kristallogr., Kristallgeom., Kristallphys., Kristallchem.* **1972,** *135,* 34-55.

[5] L. Fanfani, A. Nunzi, P. F. Zanazzi, A. R. Zanzari, *Amer. Min.* **1973,** *58,* 314-322.

[6] J. Majzlan, R. Michallik, *Min. Mag.* **2007,** *71,* 553-569.

[7] Y. Xu, K. Qin, K. Ding, Y. Miao, T. Fang, X. Xu, H. Sun, *Kuangchuang Dizhi* **2007,** *26,* 58-69.

[8] B. G. Lottermoser, *Neues Jahr. Miner.* **2005,** *181,* 183-190.

[9] B. G. Lottermoser, P. M. Ashley, *J. Geochem. Expl.* **2005,** *85,* 119-137.

[10] B. G. Lottermoser, P. M. Ashley, M. T. Costelloe, *Environ. Geol.* **2005,** *48,* 748-761.

[11] B. G. Lottermoser, M. T. Costelloe, P. M. Ashley, *Publications of the Australasian Institute of Mining and Metallurgy* **2003,** *3/2003,* 733-738.

[12] P. A. Williams, Oxide Zone Geochemistry, Ellis Horwood Ltd, Chichester, West Sussex, England, 1990.

[13] R. Atanassova, T. Kerestedjian, *Geokhimiya, Mineralogiya i Petrologiya* **2009,** *47,* 51-63.

[14] J. K. Jerz, J. D. Rimstidt, *Amer. Min.* **2003,** *88,* 1919-1932.

[15] T. Buckby, S. Black, M. L. Coleman, M. E. Hodson, *Water-Rock Interaction, Proceedings of the International Symposium on Water-Rock Interaction, 10th, Villasimius, Italy, June 10-15, 2001* **2001,** *2,* 1189-1192.

[16] T. Buckby, S. Black, M. L. Coleman, M. E. Hodson, *Min. Mag.***2003,** *67,* 263-278.

[17] R. Hakkou, M. Benzaazoua, B. Bussiere, *Mine Water and the Environment* **2008,** *27,* 145-159.

[18] J. M. Hammarstrom, R. R. Seal, A. L. Meier, J. M. Kornfeld, *Chem. Geol.***2005,** *215,* 407-431.

[19] I. Kostova, *Godishnik na Sofiiskiya Universitet "Sv. Kliment Okhridski", Geologo-Geografski Fakultet, Kniga 1: Geologiya* **2006,** *98,* 87-107.

[20] G. M. Marion, J. S. Kargel, D. C. Catling, *Geochim. Cosmochim. Acta* **2008,** *72,* 242-266.

[21] K. Omori, P. F. Kerr, *Geol. Soc. Amer. Bull.* **1963,** *74,* 709-734.
[22] P. Sobron, A. Sanz, T. Acosta, F. Rull, *Spectrochim. Acta,* **2009,** *71A,* 1678-1682.
[23] R. L. Frost, K. H. Bakon, S. J. Palmer, *J. Raman Spectrosc.* **2010,** *41,* 78-83.
[24] R. L. Frost, J. Cejka, J. Sejkora, J. Plasil, S. Bahfenne, S. J. Palmer, *J. Raman Spectrosc.* **2010,** *41,* 571-575.
[25] R. L. Frost, J. Cejka, J. Sejkora, J. Plasil, S. Bahfenne, S. J. Palmer, *J. Raman Spectrosc.* **2010,** *41,* 566-570.
[26] R. L. Frost, J. Sejkora, E. C. Keeffe, J. Plasil, J. Cejka, S. Bahfenne, *J. Raman Spectrosc.* **2010,** *41,* 202-206.
[27] R. L. Frost, P. A. Williams, W. Martens, J. T. Kloprogge, P. Leverett, *Journal of Raman Spectroscopy* **2002,** *33,* 260-263.
[28] S. D. Ross, *in The infrared spectra of minerals,* **1974,** *Chapter 18 pp 423,* The Mineralogical Society London.
[29] S. D. Ross, Inorganic Infrared and Raman Spectra (European Chemistry Series), 1972.
[30] W. Martens, R. L. Frost, J. T. Kloprogge, P. A. Williams, *J. Raman Spectrosc.* **2003,** *34,* 145-151.
[31] R. L. Frost, J. T. Kloprogge, P. A. Williams, P. Leverett, *J. Raman Spectrosc.* **2000,** *31,* 1083-1087.
[32] C. August, *Mineralogia Polonica* **1986,** *15,* 79-89.
[33] I. Bobos, N. Duraes, F. Noronha, *J. Geochem. Expl.* **2006,** *88,* 1-5.
[34] D. M. Carmona, A. Faz Cano, J. M. Arocena, *Geoderma* **2009,** *150,* 150-157.
[35] I. M. Farkas, T. G. Weiszburg, P. Pekker, E. Kuzmann, *Can. Min.* **2009,** *47,* 509-524.
[36] E. Ferreira da Silva, I. Bobos, J. Xavier Matos, C. Patinha, A. P. Reis, E. Cardoso Fonseca, *Appl. Geochem.* **2009,** *24,* 383-401.

290 **List of Figures**

291

292 Figure 1 Raman spectrum of copiapite in the 700 to 1300 cm^{-1} region

293

294 Figure 2 Raman spectrum of ferricopiapite in the 700 to 1300 cm^{-1} region

295

296 Figure 3 Raman spectrum of magnesiocopiapite in the 700 to 1300 cm^{-1} region

297

298 Figure 4 Raman spectrum of zincocopiapite in the 700 to 1300 cm^{-1} region

299

300 Figure 5 Raman spectrum of copiapite in the 100 to 700 cm^{-1} region

301

302 Figure 6 Raman spectrum of ferricopiapite in the 100 to 700 cm^{-1} region

303

304 Figure 7 Raman spectrum of magnesiocopiapite in the 100 to 700 cm^{-1} region

305

306 Figure 8 Raman spectrum of zincocopiapite in the 100 to 700 cm^{-1} region

307

308

309

310

311

312

313

314

315

316

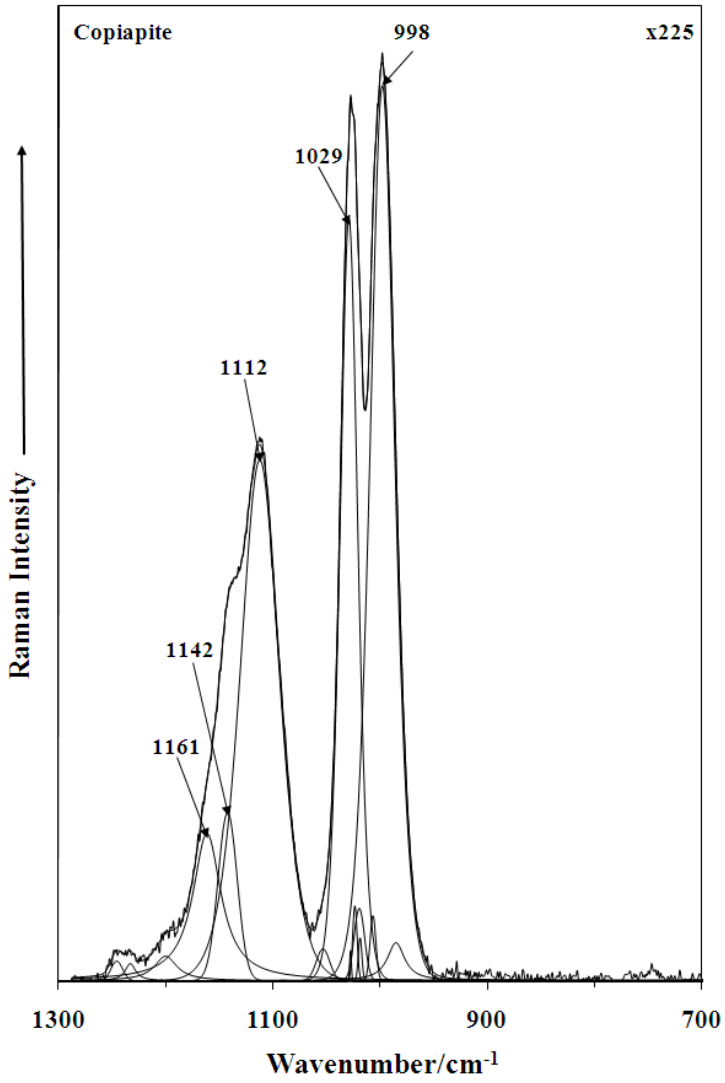

317

318

319 **Figure 1**

320

321

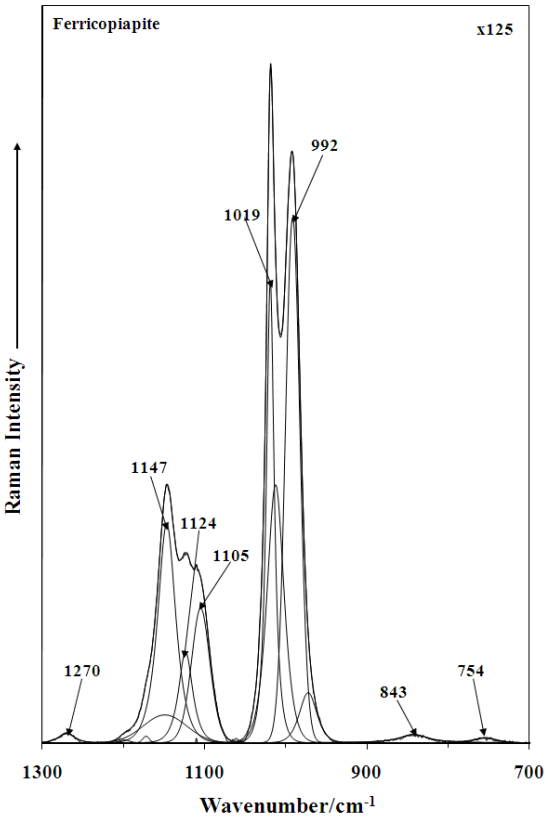

322

323

324 **Figure 2**

325

326

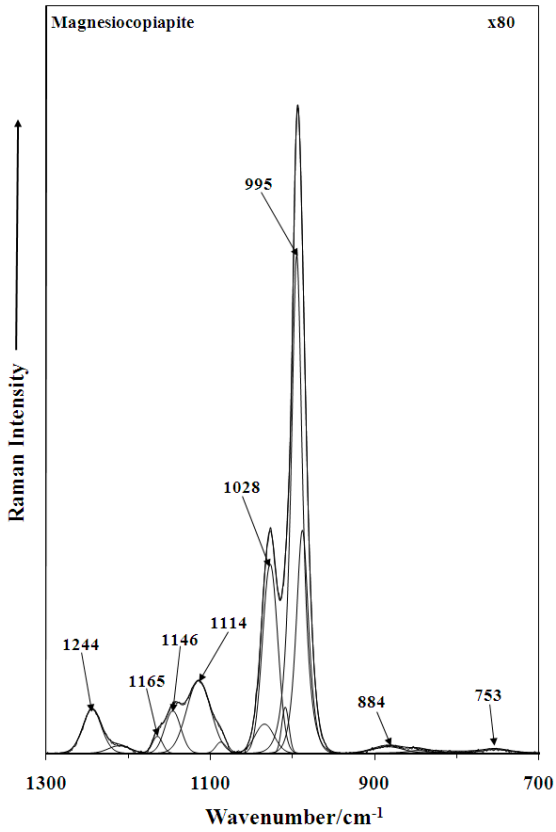
Magnesiocopiapite
x80
995
1028
1114
1146
1165
1244
884
753
Raman Intensity
1300
1100
900
700
Wavenumber/cm-1

Figure 3

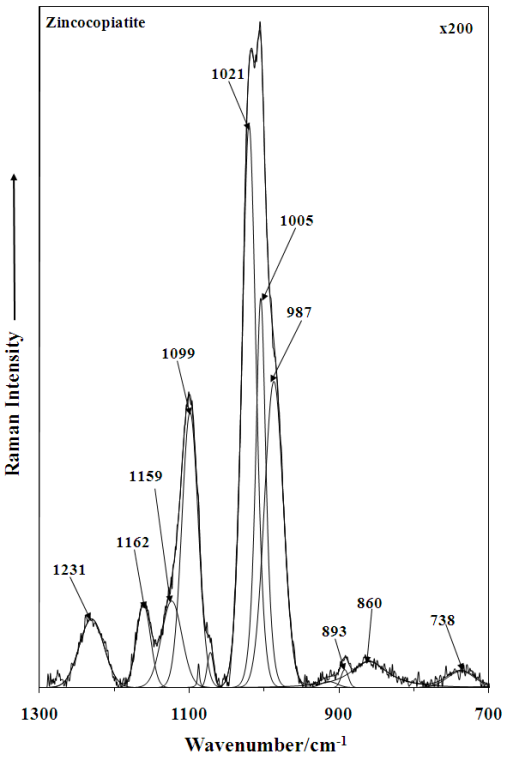
Zincocopiatite
x200
1021
1005
987
1099
1159
1162
1231
860
893
738
Raman Intensity
1300
1100
900
700
Wavenumber/cm-1

Figure 4

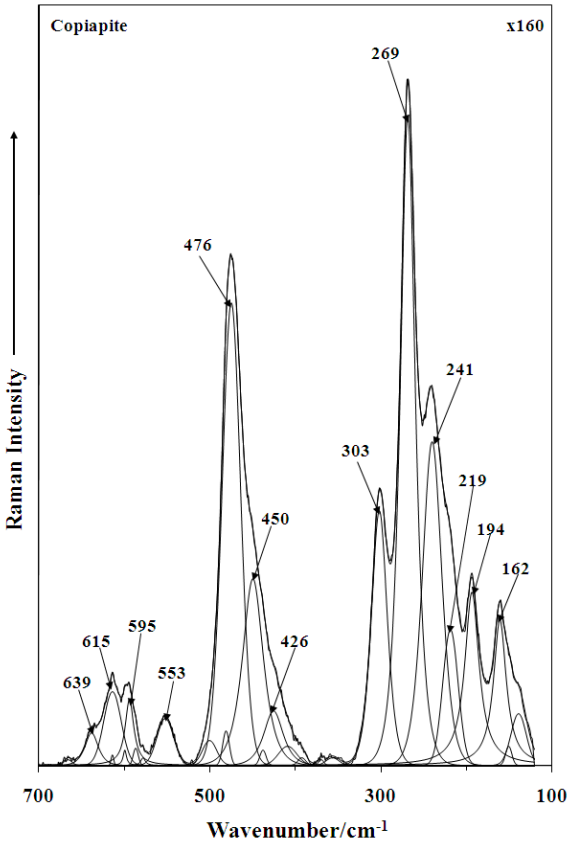

338

339

340 **Figure 5**

341

342

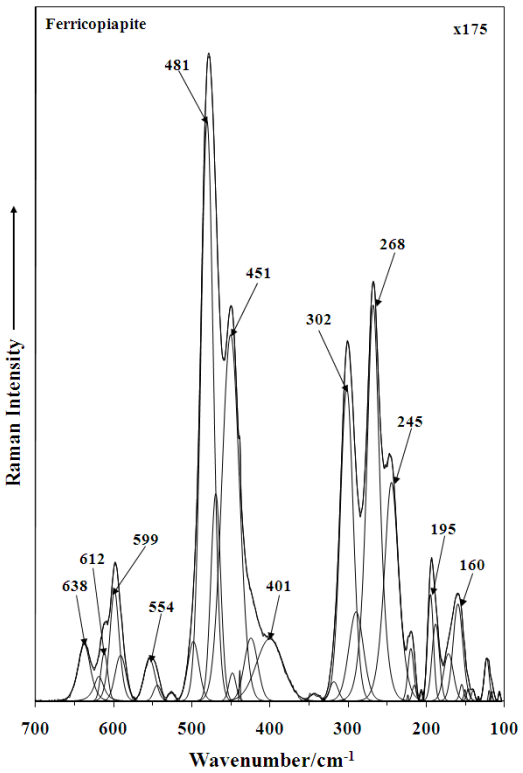

343

344

345 **Figure 6**

346

347

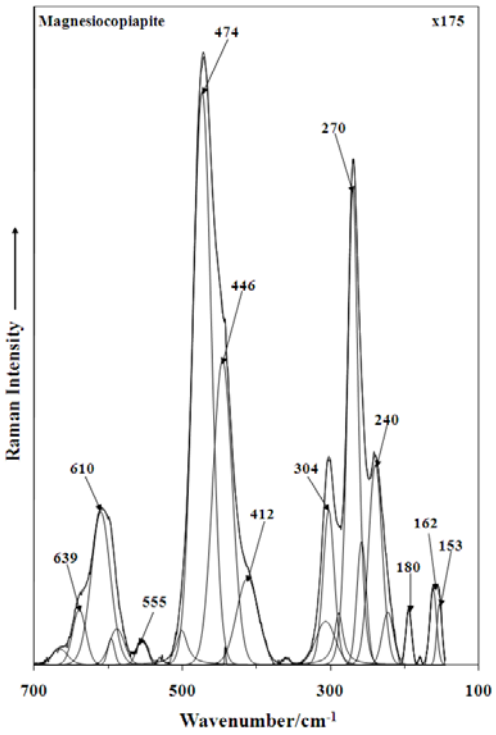
Magnesiocoplapite
x175
474
270
446
240
610
304
412
162
153
639
180
555
Raman Intensity
700
500
300
100
Wavenumber/cm-1

Figure 7

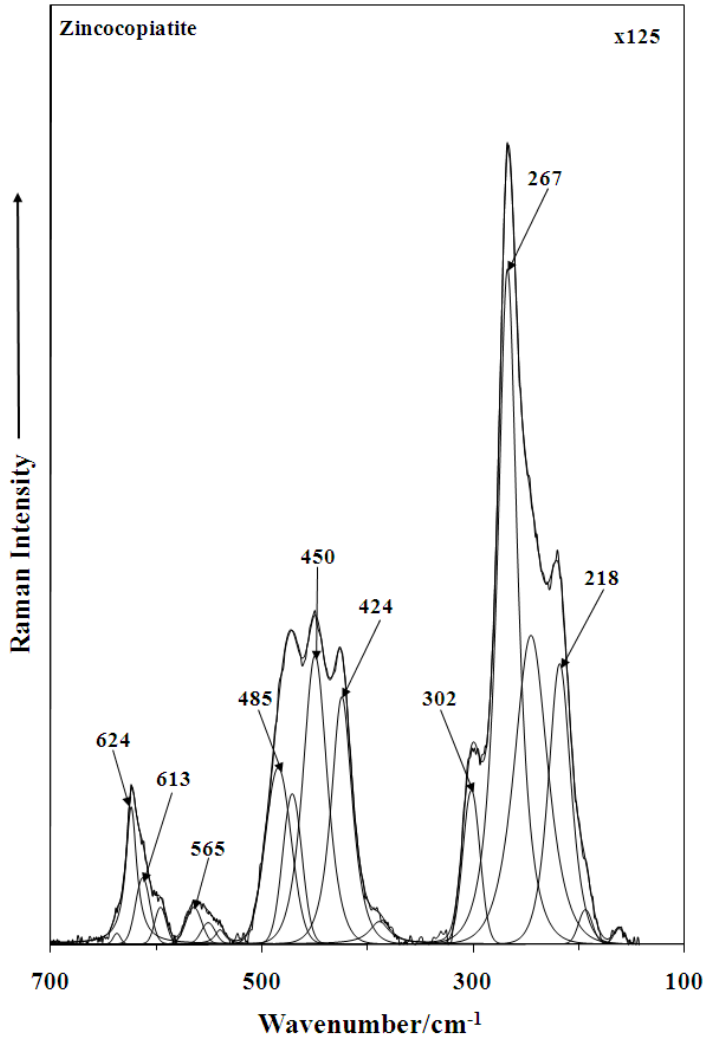

353

354

355 **Figure 8**

356